Coherent control of a semiconductor qubit in the strong coupling regime: Impact of energy and phase relaxation mechanisms

Alexandre Enderlin,[1,*] Marco Ravaro,[1,2] Valia Voliotis,[1,3] Roger Grousson,[1,2] and Xue-Lun Wang[4]
[1]*Institut des NanoSciences de Paris, Université Pierre et Marie Curie, Campus Boucicaut, 140 Rue de Lourmel, 75015 Paris, France*
[2]*Institut des NanoSciences de Paris, CNRS UMR 7588, Campus Boucicaut, 140 Rue de Lourmel, 75015 Paris, France*
[3]*Université d'Evry Val d'Essonne, Boulevard F. Mitterand, 91025 Evry, France*
[4]*Nanotechnology Research Institute, National Institute of Advanced Industrial Science and Technology (AIST), Tsukuba Central 2, Tsukuba 305-8568, Japan*

(Received 3 April 2009; revised manuscript received 10 June 2009; published 4 August 2009)

We report on coherent control of the fundamental exciton state in a single quantum dot by means of two phase-locked picosecond laser pulses. By analyzing the experiments performed in the Rabi regime and comparing them to numerical simulations, we show that we can address the exciton coherence and get an insight into the involved dephasing processes. The total decoherence time T_2 (170 ps) is comparable to the effective exciton lifetime T_1 (200 ps), although not reaching the upper theoretical limit of $2T_1$. We conclude that energy relaxation and pure dephasing processes due to virtual scattering with phonons both contribute on an equal footing to the loss of coherence in this kind of monolayer-step-induced GaAs quantum dots.

DOI: 10.1103/PhysRevB.80.085301 PACS number(s): 71.35.−y, 78.47.Fg, 78.67.Hc

I. INTRODUCTION

Coherent manipulation of quantum states is a crucial step toward quantum information processing. Semiconductor quantum dots (QDs) offer unique opportunities to investigate quantum optical effects in a solid-state system and appear as promising candidates to be the elementary bricks for quantum computing.[1] The coherent control (CC) of the excitonic polarization in a QD optically driven by a pair of phase-tailored pulses has been addressed both in the weak and in the strong coupling regimes.[2,3] In the latter one, Rabi oscillations (ROs) have been observed, thereby demonstrating the ability of manipulating a given quantum state.[4]

Of fundamental importance is the quantum coherence of the exciton, which is affected by the interaction between the QD and its environment, thus limiting the number of possible quantum operations. Decoherence mechanisms are mainly due to radiative recombination, interaction with phonons, and fluctuations of the electrostatic surrounding.[5,6] In order to take advantage of the longest possible coherence time, it is more interesting to drive the lowest lying level of the exciton since it is the least interacting state with its environment. The real challenge is however to be able to detect the emission of the resonantly excited exciton fundamental state. Despite this difficulty, ROs of this state have been demonstrated so far in guided wave geometry[7,8] or with other techniques such as differential transmission,[9] four-wave mixing,[10] and photodiode spectroscopy.[11] However, CC has been performed on the excited levels of QDs, which populate the emitting fundamental state after relaxation.[2–4] In that case, the resulting dephasing time is short, due to an additional contribution of relaxation to coherence loss.

In this paper we report and discuss CC of the truly resonantly driven fundamental exciton in a single QD. Experiments are performed on monolayer-step-induced GaAs QDs embedded in a one-dimensional waveguide. By addressing different excitation regimes, depending on pulse delay and power, we show that CC provides a useful tool not only to manipulate the excitonic state but also to measure its relaxation-time constants. A common approach used to deduce the overall dephasing time T_2 is the measurement of the homogenous broadening of the emission line, either directly,[12] or by high-resolution Fourier spectroscopy.[13] However, the physical mechanisms responsible for dipole decoherence cannot be elucidated in a straightforward manner. For instance, in Besombes *et al.*,[12] the homogeneous broadening of the QD luminescence line is attributed to strong exciton-phonon interaction leading to the formation of polarons. In Berthelot *et al.*,[13] the fluctuations of the transition energy due to Coulomb interaction with charges trapped in the vicinity of the QD explain the homogeneous broadening. Four-wave-mixing and CC experiments are techniques based on the dipole interferences and thus any long-term fluctuations leading to spectral diffusion can be singled out. In such a case, very long coherence times can be demonstrated comparable with the exciton lifetime.[14] Therefore, a clear understanding of the physical processes underlying exciton dephasing is of fundamental interest to predict and control decoherence toward applications of QDs in quantum computing.

The paper is organized as follows: in Sec. II, we introduce general concepts of CC with two identical pulses. In Sec. III, we present experimental results and numerical simulations in two limiting regimes: the case of maximum coherence obtained for $\pi/2$ pulses (Sec. III A) and the case of zero coherence obtained for π pulses (Sec. III B).The overall dephasing constant T_2 is easily determined in the first case while the second one provides the exciton lifetime T_1. As a consequence, CC experiments in different excitation regimes allow us to address both energy and pure phase relaxation mechanisms.

II. CONCEPTS OF COHERENT CONTROL

When excited near resonance, the QD can be considered as a two-level system: the $|0\rangle$ and $|1\rangle$ states stand for the

ground (vacuum, absence of electronic excitation) and the fundamental state of the confined exciton, respectively. In order to take into account the interaction of such two-level system with its environment (fluctuations of the vacuum electromagnetic field, phonons, and charges), one can use the matrix density formalism, which is based on two phenomenological relaxation constants: T_1 and T_2. The lifetime T_1 stands for the relaxation time of the excitonic population $|1\rangle$ and T_2 for the relaxation time of the field-induced coherence between the two states $|0\rangle$ and $|1\rangle$. In the $\{|0\rangle,|1\rangle\}$ basis, the density matrix ρ of a two-level system reads

$$\rho(t) = \begin{pmatrix} \sigma_{00}(t) & \sigma_{01}(t) \\ \sigma_{10}(t) & \sigma_{11}(t) \end{pmatrix}. \tag{1}$$

The diagonal terms $\sigma_{00}(t)$ and $\sigma_{11}(t)$ stand for the population of the fundamental and excited state, respectively, while the off-diagonal terms $\sigma_{01}(t)$ and $\sigma_{10}(t)$ stand for the coherence of the quantum state. The evolution of these terms is driven by the well-known optical Bloch equations.[15,16] In the following, we use this formalism to simulate and interpret coherent control experiments. Such experiments are based on the use of two laser pulses that interact successively with the QD. The laser pulse is characterized by its area θ,

$$\theta = \int_{-\infty}^{+\infty} \frac{\mu}{\hbar} E_0(t) dt, \tag{2}$$

μ being the dipole moment of the transition and E_0 the pulse electric field envelope.

The first pulse prepares a quantum superposition $\rho(t=0)$ that can be controlled by changing its area θ,

$$\rho(0) = \begin{pmatrix} \cos^2\left(\frac{\theta}{2}\right) & \frac{\sin^2\theta}{2} \\ \frac{\sin^2\theta}{2} & \sin^2\left(\frac{\theta}{2}\right) \end{pmatrix}. \tag{3}$$

Then, the exciton dipole interacts with the second pulse which, in turn, modifies the quantum superposition. This modification is driven by the area of the pulse and its phase difference with the dipole oscillation.

Here, we consider pulses with same area θ with short duration τ compared to the other relevant time constants: $\tau \ll T_1$, T_2. Physically, this means that we neglect population and coherence relaxation during the laser-matter interaction. Under this assumption, Bloch equations can be analytically solved, as shown in the Appendix. Figure 1 shows the excited-state population $\sigma_{11}(t)$ of a single QD interacting with two pulses delayed by δ. After creation of an exciton, in the time-interval $[0,\delta^-]$, the luminescence decay is exponential with the characteristic time T_1. Between δ^- and δ^+, the second pulse interacts with the two-level system and modifies its quantum state. Finally, for $t > \delta^+$, the population decays again with the same time constant T_1. The integral of this curve corresponds to the time-integrated luminescence measured experimentally.

In order to evaluate the integrated luminescence, the main task is to calculate $\sigma_{11}(\delta^+)$, the excitonic population after the interaction with the second pulse. Using the results obtained

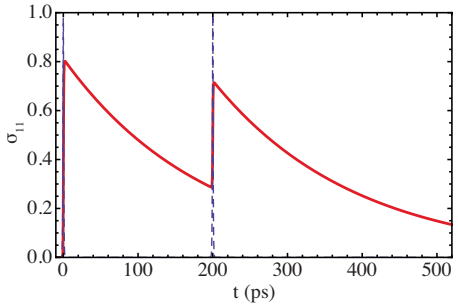

FIG. 1. (Color online). Population of the excited-state σ_{11} vs time (red solid curve) of a QD driven by two θ pulses delayed by an arbitrary δ=200 ps (blue dashed curves).

in the Appendix [see Eq. (A5)], we can write $\sigma_{11}(\delta^+)$ in the following way:

$$\sigma_{11}(\delta^+,\theta,\phi) = \sin^2\left(\frac{\theta}{2}\right) e^{-\delta^-/T_1}, \tag{4}$$

$$- \sin^2\left(\frac{\theta}{2}\right)\Delta(\delta^-), \tag{5}$$

$$+ \frac{1}{2}\sin^2\theta\cos\phi e^{-\delta^+/T_2}, \tag{6}$$

where $\Delta(\delta^-)$ is the population inversion at $t=\delta^-$, defined as $\Delta(\delta^-)=\sigma_{11}(\delta^-)-\sigma_{00}(\delta^-)$, and ϕ is the relative phase between the two pulses.

Term (4) can be interpreted as the excited-state population $\sigma_{11}(\delta^-)$ created by the first pulse just before the QD interacts with the second pulse. Term (5) expresses the variation in σ_{11} due to the incoherent part of the interaction with the second pulse. It deals with the competition between the absorption probability, proportional to the $|0\rangle$ state population, and the stimulated emission probability, proportional to the $|1\rangle$ state population. The resulting contribution to $\sigma_{11}(\delta^+)$ is proportional to the population inversion at delay δ^-, i.e., $\Delta(\delta^-)$. It is convenient to express this term as a function of $\Delta(0)$, the inversion of population induced by the first pulse, instead of $\Delta(\delta^-)$. Thus, term (5) splits in

$$\sin^2\left(\frac{\theta}{2}\right)\Delta(\delta^-) = \sin^2\left(\frac{\theta}{2}\right)\Delta(0)e^{-\delta/T_1} \tag{7}$$

$$+ \sin^2\left(\frac{\theta}{2}\right)[1-e^{-\delta/T_1}] \tag{8}$$

with

$$\Delta(0) = \sigma_{11}(0) - \sigma_{00}(0) = \sin^2\left(\frac{\theta}{2}\right) - \cos^2\left(\frac{\theta}{2}\right). \tag{9}$$

The $e^{-\delta/T_1}$ factor in term (7) and the additional repopulation term (8) arise from spontaneous emission in the interval $[0,\delta]$, which increases the absorption probability as a function of time.

Term (6) deals with the coherent part of the interaction between the exciton and the second pulse. This contribution

subsists during the coherence time of the two-level system. The cos ϕ factor accounts for the phase difference between the exciton dipole and the pulse electric field. Note that for delays $\delta \leq T_2$, two in-phase θ pulses are equivalent to one 2θ pulse.

In a CC experiment, we record the single QD luminescence as a function of the relative phase and the delay between the two pulses. The luminescence oscillates with ϕ at a given delay and the fringes contrast decays with increasing delays. In the nonlinear Rabi regime, the contrast is a function not only of the delay δ and T_2 but depends as well on T_1 and θ.

III. EXPERIMENTAL RESULTS

The studied QDs are naturally formed by monolayer thickness fluctuations at the heterointerfaces of a GaAs/GaAlAs quantum wire grown by metal-organic vapor-phase epitaxy on a nonplanar GaAs substrate.[17] The QDs are elongated along the free axis of the quantum wire and their typical length ranges between 10 and 100 nm.[18] Since the confinement potential is quite weak, only one or a few discrete states are confined in each dot, depending on its size. In order to address the fundamental exciton state at resonance, the dots are embedded in a one-dimensional monomode waveguide built from several GaAlAs layers with different aluminum concentrations. The waveguiding geometry has several advantages: first, due to the spatial confinement of light, the coupling with the QDs is enhanced. Second, the laser light propagation direction is perpendicular to the luminescence detection direction. Indeed, the single QD luminescence is collected from the waveguide top surface by a confocal microphotoluminescence (μPL) detection setup.[19] Moreover, in these nonplanar structures which are grown on a V-grooved substrate, the optical mode is well confined in the bottom of the V-shaped layers, a few microns far from the top surface. Since the laser light is contained in the guided mode, the scattered light is greatly suppressed and the resonant luminescence is almost background free, at low pump power. However, under strong excitation, laser scattering remains a severe limitation for the observation of resonant RO.[7] The ps excitation pulses are provided by a Ti-sapphire laser and the pair pulses are generated using a stabilized Michelson interferometer, which allows controlling their relative optical phase on a scale of $\lambda/100$.[20] The spatial resolution of the setup is diffraction limited to 1 μm^2. The spectral resolution, 40 μeV, is not sufficient to measure the narrow linewidth of the QD emission, thus preventing the estimate of the corresponding dephasing time T_2. The optical eigenmodes of the waveguide and the QD eigenstates are both linearly polarized. Thus, for low pump power, the QD μPL and the laser are, as expected, copolarized. Measurements are performed at 10 K.

A. Dephasing processes

In this section we focus on the case of $\pi/2$ pulses, which maximizes quantum interferences [term (6)]. Indeed, the coherence of a quantum state prepared with a $\pi/2$ pulse [$|\psi\rangle = \frac{1}{\sqrt{2}}(|0\rangle + |1\rangle)$] has a maximum amplitude equal to 1/2. Moreover, since the fundamental and excited-state populations are equal, i.e., $\Delta(0)=0$, the absorption and stimulated emission processes cancel each other. Thus, the two terms driving the fringe visibility are the repopulation term (8), which resets the excited-state population $\sigma_{11}(\delta^+)$ to its initial value 1/2 and the interference term (6). The resulting population after interaction with the second pulse reads

$$\sigma_{11}(\delta^+, \theta = \pi/2, \phi) = \frac{1}{2}(1 + \cos\phi e^{-\delta/T_2}). \qquad (10)$$

Then, the population oscillates as a function of ϕ at a given delay as shown in the inset of Fig. 2(a). The open (solid) circles show the experimental μPL intensity from a single QD as a function of the delay between the two driving in-phase (out-of-phase) pulses. They represent the upper and lower envelopes of the interference fringes. Data dispersion stems from μPL intensity fluctuations due to mechanical

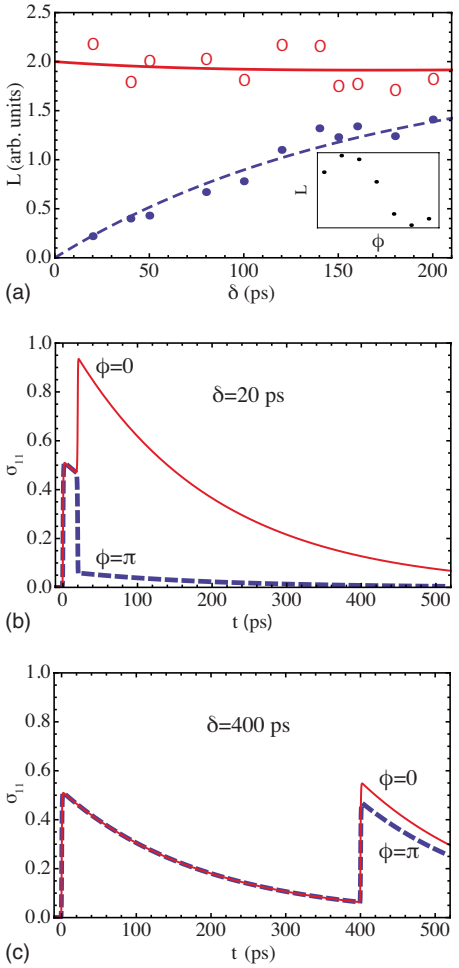

FIG. 2. (Color online) (a) μPL intensity L vs delay δ for $2\pi/2$ in-phase (red open circles) and out-of-phase (blue solid circles) pulses. The corresponding theoretical curves (solid and dashed lines, respectively) are calculated for $T_2=170$ ps (see Fig. 3). Inset: time-integrated (10 s) μPL intensity vs ϕ for a fixed delay. [(b) and (c)] Calculated $\sigma_{11}(t)$ for two in-phase (red solid curves) and out-of-phase (blue dashed curves) pulses ($T_1=200$ ps and $T_2=170$ ps).

drifts or laser power fluctuations during the long-term data acquisition. However, this effect does not influence the contrast, as shown below. Solid lines on Fig. 2(a) represent the theoretical curves obtained from Eqs. (A5) and (A6), whose expression as a function of the delay and relative phase between the pulses reads

$$L(\delta,\phi) = \frac{T_1}{2}(2 - e^{-\delta/T_1} + \cos\ \phi e^{-\delta/T_2}). \tag{11}$$

At variance with the weak-coupling regime,[2] here the envelopes are not symmetric: the maximum is nearly constant whereas the minimum increases monotonically from 0 toward the maximum envelope at longer delays. For short delays [Fig. 2(b)], the time-resolved luminescence depends mainly on the relative phase between the two pulses. From a microscopic point of view, the exciton photocreated by the first pulse has not lost its phase memory yet, resulting in a strongly phase-dependent interaction with the second pulse. If the dipole oscillates in phase with the electric field of the second pulse, then constructive interferences occur turning the $\pi/2$ state into a π state (red solid curve). In the case of phase opposition, destructive interferences annihilate the dipole oscillation (blue dashed curve).

On the contrary, for long delays, the time-resolved luminescence is nearly phase independent. Indeed, the integrals in the $\phi=0$ and $\phi=\pi$ cases [red and blue curves on Fig. 2(c)] are almost equal, the small difference arising from residual interferences. The main term driving σ_{11} at $t=\delta$ is repopulation, which is phase independent. The exciton created by the first pulse has a high probability to recombine and the interaction with the second pulse creates an identical exciton. Accordingly, in this incoherent regime the luminescence signal does not strongly depend on the phase and it is maximum for two in-phase pulses at $\delta=0$.

The comparison of the two above regimes reveals that the time-integrated luminescence for in-phase pulses [red solid curves in Figs. 2(b) and 2(c)], for short and long delays is almost equal. This is consistent with the slow variation in the upper envelope of the interference fringes [Fig. 2(a)]. On the contrary, this is not the case for two out-of-phase pulses. In addition to these regimes, a third one can exist, for which the QD is "transparent." This phenomenon occurs each time an exciton has lost its phase memory without relaxing, after a pure dephasing process.[5] In this case, the second pulse can neither interfere with the dipole, as it has lost its coherence, nor create a second exciton, as the first one has not yet relaxed. In that case, everything goes as if the second pulse was not interacting with the QD.

The fringe visibility is defined by Eq. (A7) and the contrast for $\pi/2$ pulses reads, using Eqs. (A5) and (A6),

$$C(\delta) = \frac{e^{-\delta/T_2}}{2 - e^{-\delta/T_1}}. \tag{12}$$

The experimental results are shown in Fig. 3 from the data presented in Fig. 2(a). As previously mentioned, in the nonlinear Rabi regime, the contrast depends on T_2 but also on T_1. In order to fit the experimental data, the value of T_1 was fixed to 200 ps, as measured by time-resolved μPL experiments (not shown here), T_2 being the only fitting parameter. It is worth noticing that the resonant radiative lifetime measured in our experiments is modified by the particular electromagnetic environment due to the presence of the waveguide. The coupling to the guided mode enhances the spontaneous emission process, reducing the lifetime. Similar results have been reported by Kuroda *et al.*[21]

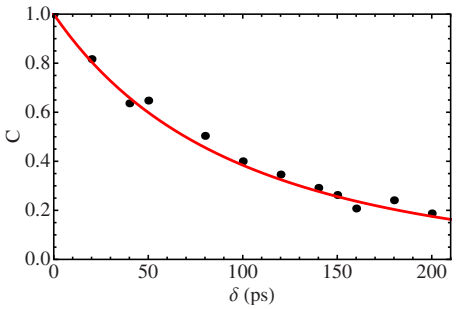

FIG. 3. (Color online) Quantum interference contrast as a function of delay δ (solid circles) fitted with Eq. (12) for fixed T_1 = 200 ps (solid red line). The dephasing time obtained is T_2 = 170 ps.

By fitting the experimental data we deduce a coherence time $T_2=170$ ps, comparable with the exciton lifetime, although shorter than the upper theoretical limit $2T_1$. This implies that pure dephasing processes are also involved. The total dephasing rate can be written as $\frac{1}{T_2}=\frac{1}{2T_1}+\frac{1}{T_2^*}$, where $1/T_1$ is the energy relaxation rate and $1/T_2^*$ the pure dephasing term.

The first term accounts for inelastic scattering due to spontaneous emission of photons and absorption or emission of phonons that change the exciton final state. Thus, T_1 can be identified as the effective lifetime of the exciton. The contribution due to inelastic scattering with acoustic phonons has been calculated for similar QDs as a function of the QD length.[22] In the case of the ground exciton state, only phonon absorption has to be taken into account. The calculations show that at 10 K, the coupling between the ground exciton state and the first excited state in the dot occurs over long-time scales ranging between 1.5 and 0.5 ns for 35- and 45-nm-long QDs, respectively, which are typical lengths for this kind of QDs.[23] Moreover, we do not observe emission from excited states when pumping at resonance the ground exciton state, contrary to recently reported results.[24] Thus, relaxation by phonons is not very efficient and in our case the effective lifetime is limited only by photons emission. For longer QDs, the exciton lifetime is mainly limited by the coupling with the phonon bath while for shorter lengths, the oscillator strength is not sufficient and the system cannot undergo Rabi oscillations.

The second term, corresponding to the pure dephasing term, originates from elastic scattering due to interactions with virtual phonons,[5] polarons,[12] or environmental fluctuating charges,[13] which leave the exciton in the same state but modify its phase. In the case discussed here, $T_2^*=270$ ps, so the probability of having pure dephasing is as important as the spontaneous emission probability. It is worth noticing that a CC experiment, whose relevant time scale is T_2, is not sensitive to charge fluctuations which occur on a much

longer time scale on the order of 1 ms. In addition, due to low enough temperature, we can exclude the presence of polarons as well, as confirmed by the absence of lateral wings in the emission line shape. Therefore, the pure dephasing contribution is due to virtual phonon-scattering mechanisms.

Finally, we may notice that in the weak-coupling regime the general formula for the contrast given by Eq. (12) can be expanded in the limit $\theta \ll \pi$ and becomes a simple exponential decay

$$C(\delta) = e^{-\delta/T_2}, \tag{13}$$

matching the results obtained by Fedorov *et al.*[25] However, this regime does not allow to fully manipulate the population of a quantum superposition.[2] Only in the strong coupling regime, does CC become a powerful tool to manipulate both the population and the coherence of a quantum superposition.

B. Radiative recombination

In the case of a pure π state, the coherence term is vanishing so that the relative phase ϕ does not play any role. The luminescence, L, only depends on the energy relaxation-time T_1 and so CC experiments with π pulses allow us to measure the effective lifetime of excitons. Figure 4(a) shows the μPL intensity from the same QD investigated above, recorded versus the delay between the two π pulses. Since the integrated μPL signal is proportional to the exciton population, by using the general relations (4)–(9) for π pulses, we obtain

$$\sigma_{11}(\delta, \theta = \pi, \phi) = 1 - e^{-\delta/T_1}, \tag{14}$$

$$L(\delta) = 2T_1(1 - e^{-\delta/T_1}). \tag{15}$$

The effect of a sequence of two π pulses can then be easily understood: after the first exciton has been created, the second pulse can either stimulate the emission of a photon or create an identical exciton in the same state, depending on the delay δ as compared to T_1. For delays shorter than T_1 [Fig. 4(b)] the stimulated emission is predominant and the residual luminescence is due to the finite recombination probability. On the contrary, for delays much longer than T_1, the first exciton has recombined and the second pulse repopulates the system. The integrated luminescence signal for any delay $\delta > T_1$ is then directly proportional to the exciton recombination probability at time $t = \delta$. This can be observed in Fig. 4(c), where the probability to create an exciton is high for both pulses and the resulting time-integrated luminescence intensity is twice than for a single pulse. By fitting experimental data in Fig. 4(a) with Eq. (15), we obtained an effective lifetime of 200 ps, in satisfactory agreement with the time-resolved μPL results. CC in this excitation regime then becomes an interesting method to measure lifetimes especially in wavelength domains where specific detectors have not yet been developed.

IV. CONCLUSION

Coherent control in the strong coupling regime is demonstrated on the fundamental exciton transition of a single monolayer-step-induced GaAs QD. The dephasing time T_2 as well as the effective lifetime T_1 can be measured in this regime by using phase-locked pairs of $\pi/2$ and π optical pulses, respectively. In this kind of samples, only QDs with lengths ranging around 40 nm, corresponding to an oscillator strength of 40, can reach the strong coupling regime and exhibit RO because of the competition between radiative decay and relaxation by phonon absorption. In this case, we measure an exciton lifetime T_1 of about 200 ps and an overall dephasing time T_2 of the same order of magnitude. We conclude that in this situation, the probability of pure dephasing processes due to virtual absorption and/or emission of phonons is comparable to that of spontaneous emission.

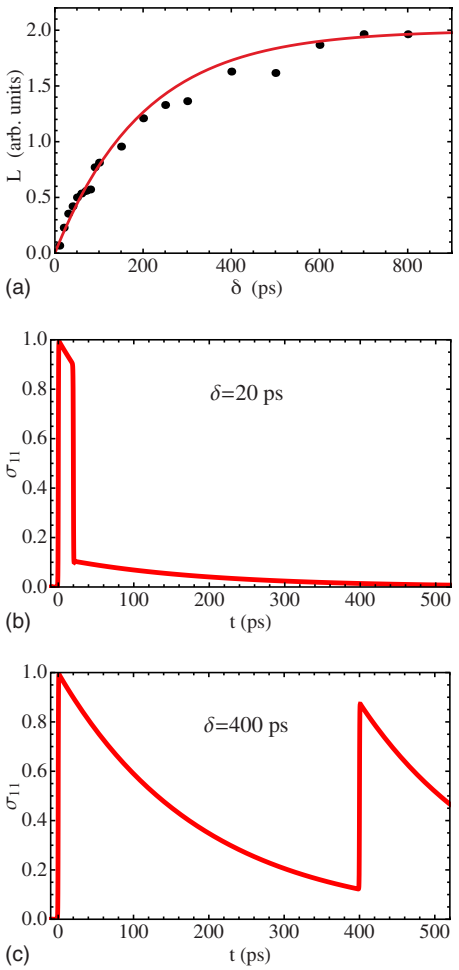

FIG. 4. (Color online) (a) μPL intensity L vs delay δ for two π pulses: experimental data (solid symbols) and fit with Eq. (15) (solid line), giving $T_1 = 200$ ps. [(b) and (c)] Calculated excited-state population σ_{11} vs time for $\delta = 20$ ps and $\delta = 400$ ps, respectively.

APPENDIX: BLOCH EQUATIONS SOLUTION IN THE CASE OF A SHORT PULSE

The purpose of this appendix is to demonstrate expressions (4)–(8) for the exciton population $\sigma_{11}(\delta^+)$ just after interaction with the second pulse. While at any other time

$\sigma_{11}(t)$ undergoes a free evolution, simply described by an exponential decay, its variation during the second pulse is not trivial to evaluate. In order to account for the perturbation of the pulse electromagnetic field, Bloch equations have to be solved in the time-interval $[\delta^-, \delta^+]$ during which this interaction takes place. With this aim, the two following assumptions are made: first, an excitation pulse resonant with the fundamental transition and second, a pulse duration much shorter than the relaxation constants T_1 and T_2 are considered. Therefore, every relaxation term in the Bloch equations can be neglected and, over the exciton characteristic time scale, a Dirac pulse can be assumed (i.e., $\delta=\delta^-=\delta^+$). Under these assumptions, the two following equations hold: $\sigma_{00}+\sigma_{11}=1$ and $\sigma_{10}=-\sigma_{01}$, where σ_{00} and σ_{11} are real quantities while the coherence terms are purely imaginary. Then, the following set of two coupled differential equations has to be solved:

$$\dot{\sigma_{11}}(t) = -\Omega(t)\sigma_{10}(t) \tag{A1}$$

$$\dot{\sigma_{10}}(t) = \Omega(t)\left[\sigma_{11}(t) - \frac{1}{2}\right].$$

We have set $\Omega(t)=\frac{\mu}{\hbar}E_0(t)$, where $E_0(t)$ is the envelope of the electric field. The initial conditions are the following:

$$\sigma_{11}(\delta^-) = \sigma_{11}(0)e^{-\delta/T_1} \tag{A2}$$

$$\sigma_{10}(\delta^-) = \sigma_{10}(0)e^{-\delta/T_2}\cos\phi,$$

where $\sigma_{11}(0)[\sigma_{10}(0)]$ is the excited-state population (coherence term) induced by the first pulse. By substitution, we obtain

$$\sigma_{11}(\delta^-) = \sin^2\left(\frac{\theta}{2}\right)e^{-\delta/T_1} \tag{A3}$$

$$\sigma_{10}(\delta^-) = \frac{\sin\theta}{2}e^{-\delta/T_2}\cos\phi$$

with

$$\theta = \int_{-\infty}^{+\infty}\Omega(t')dt', \tag{A4}$$

Finally, integration of Eq. (A1) gives

$$\sigma_{11}(\delta^+) = \frac{1}{2} + \left[\sin^2\left(\frac{\theta}{2}\right)e^{-\delta/T_1} - \frac{1}{2}\right]\cos\theta + \left[\frac{1}{2}\sin\theta e^{-\delta/T_2}\cos\phi\right]\sin\theta. \tag{A5}$$

The following step is to calculate the integrated luminescence $L(\delta,\theta,\phi)$. Knowing $\sigma_{11}(\delta,\theta,\phi)$, we can easily derive L:

$$L(\delta,\theta,\phi) = \sin^2\left(\frac{\theta}{2}\right)\int_0^{\delta}e^{-t/T_1}dt + \sigma_{11}(\delta,\phi)\int_0^{+\infty}e^{-t/T_1}dt. \tag{A6}$$

Finally, an analytical expression for the contrast can be found, which is given by

$$C(\delta,\theta) = \frac{L(\delta,\theta,0) - L(\delta,\theta,\pi)}{L(\delta,\theta,0) + L(\delta,\theta,\pi)}. \tag{A7}$$

*enderlin@insp.jussieu.fr

[1] S. Lloyd, Science **261**, 1569 (1993); C. H. Bennett and D. P. DiVincenzo, Nature (London) **404**, 247 (2000); P. Chen, C. Piermarocchi, and L. J. Sham, Phys. Rev. Lett. **87**, 067401 (2001); E. Biolatti, R. C. Iotti, P. Zanardi, and F. Rossi, *ibid.* **85**, 5647 (2000).

[2] N. H. Bonadeo, J. Erland, D. Gammon, D. Park, D. S. Katzer, and D. G. Steel, Science **282**, 1473 (1998).

[3] H. Kamada, H. Gotoh, J. Temmyo, T. Takagahara, and H. Ando, Phys. Rev. Lett. **87**, 246401 (2001).

[4] H. Htoon, T. Takagahara, D. Kulik, O. Baklenov, A. L. Holmes, Jr., and C. K. Shih, Phys. Rev. Lett. **88**, 087401 (2002).

[5] T. Takagahara, Phys. Rev. B **60**, 2638 (1999).

[6] H. Kamada and T. Kutsuwa, Phys. Rev. B **78**, 155324 (2008).

[7] R. Melet, V. Voliotis, A. Enderlin, D. Roditchev, X. L. Wang, T. Guillet, and R. Grousson, Phys. Rev. B **78**, 073301 (2008).

[8] A. Muller, E. B. Flagg, P. Bianucci, X. Y. Wang, D. G. Deppe, W. Ma, J. Zhang, G. J. Salamo, M. Xiao, and C. K. Shih, Phys. Rev. Lett. **99**, 187402 (2007).

[9] T. H. Stievater, X. Li, D. G. Steel, D. Gammon, D. S. Katzer, D. Park, C. Piermarocchi, and L. J. Sham, Phys. Rev. Lett. **87**, 133603 (2001).

[10] B. Patton, U. Woggon, and W. Langbein, Phys. Rev. Lett. **95**, 266401 (2005).

[11] S. Stufler, P. Ester, A. Zrenner, and M. Bichler, Phys. Rev. B **72**, 121301(R) (2005).

[12] L. Besombes, K. Kheng, L. Marsal, and H. Mariette, Phys. Rev. B **63**, 155307 (2001).

[13] A. Berthelot, I. Favero, G. Cassabois, C. Voisin, C. Delalande, Ph. Roussignol, R. Ferreira, and J. M. Gerard, Nat. Phys. **2**, 759 (2006).

[14] P. Borri, W. Langbein, S. Schneider, U. Woggon, R. L. Sellin, D. Ouyang, and D. Bimberg, Phys. Rev. Lett. **87**, 157401 (2001).

[15] C. Cohen Tannoudji, J. Dupont-Roc, and G. Grynberg, *Atom-Photon Interactions: Basic Processes and Applications* (Wiley, New York, 1992).

[16] L. Mandel and E. Wolf, *Optical Coherence and Quantum Optics* (Cambridge University Press, Cambridge, 1995).

[17] J. Bellessa, V. Voliotis, R. Grousson, X. L. Wang, M. Ogura, and H. Matsuhata, Appl. Phys. Lett. **71**, 2481 (1997); X. L. Wang, M. Ogura, and H. Matsuhata, *ibid.* **67**, 804 (1995).

[18] T. Guillet, R. Grousson, V. Voliotis, X. L. Wang, and M. Ogura, Phys. Rev. B **68**, 045319 (2003).

[19] R. Melet, R. Grousson, V. Voliotis, and X.-L. Wang, Phys. Status Solidi B **245**, 1098 (2008).

[20] M. U. Wehner, M. H. Ulm, and M. Wegener, Opt. Lett. **22**, 1455

(1997).
[21] K. Kuroda, T. Kuroda, K. Watanabe, T. Mano, K. Sakoda, G. Kido, and N. Koguchi, Appl. Phys. Lett. **90**, 051909 (2007).
[22] T. Guillet, Ph. D. thesis, Universite Pierre et Marie Curie, Paris, 2002; http://tel.cnrs.ccd; X. L. Wang and V. Voliotis, J. Appl. Phys. **99**, 121301 (2006).
[23] J. Bellessa, V. Voliotis, R. Grousson, X.-L. Wang, M. Ogura, and H. Matsuhata, Phys. Rev. B **58**, 9933 (1998).
[24] E. B. Flagg, J. W. Robertson, S. Founta, W. Ma, M. Xiao, G. J. Salamo, and C. K. Shih, Phys. Rev. Lett. **102**, 097402 (2009).
[25] A. V. Fedorov, A. V. Baranov, and Y. Masumoto, Opt. Spectrosc. **92**, 732 (2002).